Different aspects of laboratory analog of tropical cyclone

Different aspects of laboratory analog of tropical cyclone

A Sukhanovskii[a], A Evgrafova, A Pavlinov, E Popova and V. Shchapov

Institute of Continuous Media Mechanics UB RAS, 1, Acad. Korolev St., Perm, 614013, Russia

E-mail: [a]san@icmm.ru

Abstract. Localized heating in the rotating layer of fluid leads to the formation of intense cyclonic vortex. Cyclonic vortex becomes unstable at low values of viscosity and fast rotation of the experimental model. The instability of the vortex is tightly connected with a structure of the radial inflow. For moderate values of rotational Reynolds number Re the radial flows consist of several branches which transport angular momentum to the center of the model. When Re exceeds critical value (about 23) radial inflow changes its structure and appears as one wide branch which does not reach the center. As a result of strong anisotropy of radial inflow the cyclonic vortex is formed at some distance from the center. Further increase of Re leads to chaotic state with several vortices which appear at different locations near the periphery of the heating area. The map of regimes with stable and unstable vortices is presented.

1. Introduction

Despite decades of research the problem of tropical cyclogenesis is unsolved and attracts close attention from many scientific groups. The complexity of the problem forces researchers to study tropical cyclogenesis step by step seeing as a main goal the theory that would describe all stages of the tropical cyclone formation. For example deep convection in tropical depressions, including the effects of boundary-layer wind structure, ambient vertical and horizontal vorticity were studied in a series of idealized numerical experiments (see for example [1] and references therein).

Development and intensification of tropical cyclones (TCs) strongly depend on heat and angular momentum fluxes in the boundary layer (BL). The structure of BL is very complex and consists of secondary flows of different scales [2]. Unstable stratification increases BL rolls circulation because convective instability tends to support dynamic instability [3]. The existence of horizontal rolls of large wavelength ($\sim$ 10 km) can be explained by wave triad interaction [3]. Spiral rainbands represent another type of secondary flows of larger scale which exist in tropical cyclones. The recent review of different hypotheses which explain the dynamics and nature of inner spiral bands can be found in [4]. In [5] it was found that inner rainbands are convective clouds advected by tropical cyclone wind and deformed into spiral shapes. The role of spiral bands in transport of angular momentum and heat is still under active discussion.

Open problem is a link between wind velocity and latent heat release during formation of TCs [6, 7]. The TCs are dangerous natural hazards that cause multiple human losses and vast economical damage. The main problem is long-term reliable forecast [8]. The quality of

prediction of tropical cyclone intensity and track of its motion strongly depends on the choice of mathematical models. Up to now capabilities of numerical modeling are restricted. Most of numerical simulations are carried out using spatial resolution of 2-3 km with parametrization of the subgrid processes. Some effects like the influence of secondary flows with characteristic scale of 1-3 km on heat and mass transfer are either parametrized or neglected. Another serious problem for numerical modeling is a large number of parameters (humidity, compressibility, physical properties of media and many others). Taking into account that the time of one full-scale 3D run is one week or more, the role of all parameters is hardly possible to study. Limited capabilities of direct numerical modeling of atmospheric flows increase interest to the laboratory modeling of geophysical processes. Promising laboratory model of hurricane-like vortex was proposed in [9] that was further developed and successfully used in [10, 11, 12].

Presented paper considers different aspects of laboratory model of TC including non-stationary early phase. The approach which integrates measuring and computational resources for experimental study of latent heat release in the laboratory analog of tropical cyclone is described.

The paper is organized as follows. In section 2 we describe the experimental setup and measurement technique. Experimental results are presented in section 3 and conclusions are given in section 4.

2. Experimental setup

Experimental model is a cylindrical vessel of diameter $D = 300$ mm, and height $H = 40$ mm (figure 1(a)). The sides and bottom were made of plexiglass with a thickness 3 mm and 20 mm respectively. There was no cover or additional heat insulation at the sidewalls. The heater is a brass cylindrical plate mounted flush with the bottom. The diameter of the plate d is 104 mm, and its thickness is 10 mm. The brass plate is heated by an electrical coil placed on the lower side of the disc. Massive heater provides uniform heating which is optimal for vortex excitation. Cylindrical vessel was placed on a rotating horizontal table. Silicon oils with different values of kinematic viscosity, PMS-20, PMS-10 and PMS-5 (20, 10 and 5 cSt at at T = 25 ^{0}C) were used as working fluids. In all experiments, the depth of the fluid layer h was 30 mm and the surface of the fluid was open. The room temperature was kept constant by air-conditioning system, and cooling of the fluid was provided mainly by the heat exchange with surrounding air on the free surface and some heat losses through sidewalls. The velocity field measurements were made with a 2D particle image velocimetry (PIV) system Polis and the software package Actual Flow. The PIV velocity measurements were accurate to within 5%, estimated from calibration experiments in solid body rotation and long time series. Along with the dimensional parameters (heat flux, rotation rate and kinematic viscosity) we use the set of the non-dimensional parameters. These are the flux Grashof number Gr_f, rotational Reynolds number Re and Prandtl number Pr:

$$Gr_f = \frac{g\beta h^4 q}{c\rho\kappa\nu^2} \tag{1}$$

$$Re = \frac{\Omega h^2}{\nu} \tag{2}$$

$$Pr = \frac{\nu}{\kappa} \tag{3}$$

where g is the gravitational acceleration, h is the layer depth, β is the coefficient of thermal expansion, c is the thermal capacity, ρ is the density, ν is the coefficient of kinematic viscosity and κ is the thermal diffusivity, q is a heat flux ($q = P/S_h$, P is the power of the heater and S_h is the heater's surface area).

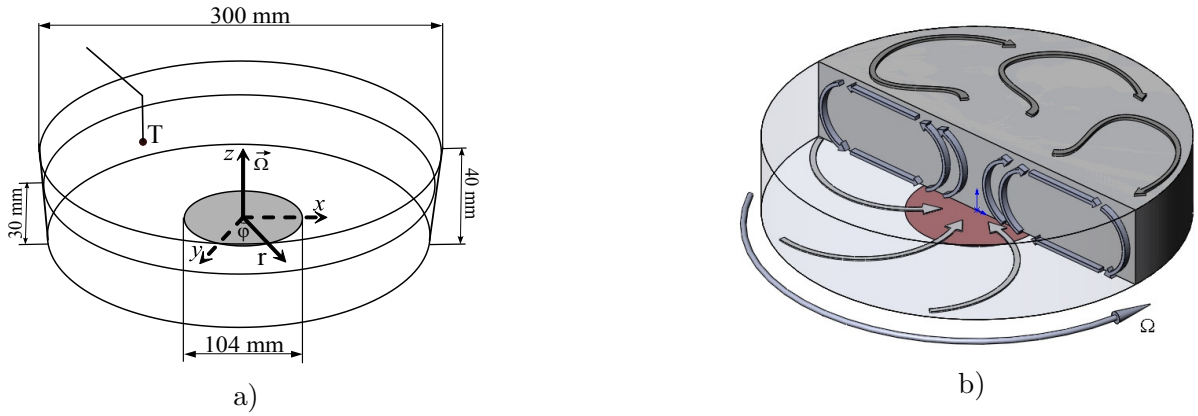

Figure 1. a - experimental model, dimensions and location of the coordinate system. T - thermocouple for control of the mean temperature; b - scheme of large-scale circulation.

Experiment with a feedback requires real-time data processing. In order to solve this problem we use supercomputer for PIV images processing. The variation of number of computational nods allows to achieve necessary rate of image processing. Essential feature of the proposed experiment is a linkage between heating and velocity of the fluid. Boundary condition on the heated surface is controlled by copper-constantan thermocouple. Thermocouple is located inside heat exchanger near the surface and it is connected with temperature regulator Termodat-17E5. It allows to set required temperature or heating power remotely. Software which controls heating power is linked with the main block providing integration of all parts of experimental system. For each experimental realization we set functional dependence between velocity of the flow and power of the heating (or temperature of the heater). Flow characteristics obtained by real-time PIV processing serve as input parameters for the heating system. Details of the developed approach can be found in [13].

3. Results

3.1. Stability of laboratory analog of TC

Detailed description of the basic flow structure can be found in [11] and here we present only brief description of the general structure of the large-scale flow. The heat flux in the central part of the bottom is a source of the intensive upward motion above the heater. Warm fluid cools at the free surface and moves toward the periphery where the cooled fluid moves downward along the side wall. Large-scale advective flow occupies the whole vessel (figure 1(b)).

The cyclonic vortex formation in the laboratory system can be described by following scenario. Large-scale radial circulation leads to the angular momentum transport and the angular momentum exchange on the solid boundaries. Convergent flow in the lower layer brings the fluid parcels with large values of angular momentum from the periphery to the center and produces cyclonic motion (figure 1(b)), lower horizontal cross-section). In the upper layer situation is opposite - divergent flow takes the fluid with low values of angular momentum to the periphery resulting in anticyclonic motion (figure 1(b), upper horizontal cross-section). Friction in the viscous boundary layers leads to the sink of angular momentum in the part of the bottom occupied by cyclonic flow and produces source of angular momentum on the sidewalls when anticyclonic flow comes to the periphery. Zero net angular momentum flux on the solid boundaries is the necessary condition for the steady-state regime [10]. The general structure of laboratory vortex (figure 2) is similar to the observational data [14] excluding the side wall area.

Series of experiments [15, 11, 12] showed that stable localized cyclonic vortex exist in a narrow range of governing parameters. Vortex becomes unstable at low value of viscosity and

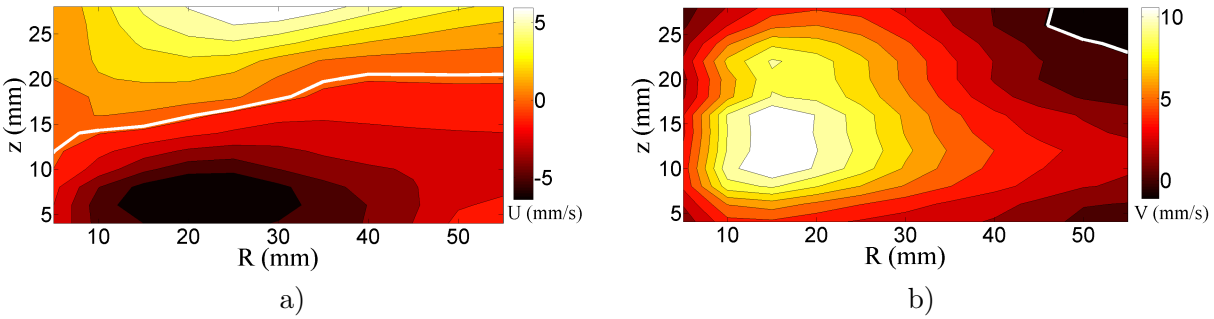

Figure 2. Mean radial (a) and azimuthal (b) velocity fields in a vertical cross-section over heating area, $Gr_f = 1.4 \cdot 10^7$, $Re = 15.6$. Thick solid white line shows the border between positive and negative values of velocity.

fast rotation of the model. Examples of instantaneous vector velocity field and streamline flow fields for the stable and unstable cases are shown in figure 3. In the case of developed cyclonic vortex there are several branches of radial inflow that comes very near to the center of the model figure 3 (left). Radial inflow transports angular momentum from the large radii to the small radii and its symmetry or asymmetry strongly influences the vortex structure. This result is in a good agreement with numerical simulation [10]. Increasing of rotational Reynolds number (2) by decreasing of viscosity or increasing of rotation rate leads to the instability of radial inflow. It changes its structure as shown in figure 3 (right). Instead of several branches which provide inflowing from different directions it is transformed into one big spiral branch that does not reach the center. As a result of this asymmetrical flux of angular momentum a localized cyclonic vortex is formed at some distance from the center. Radial inflow and cyclonic vortex slowly precessed around axis of rotation and in the mean vector field it appears as a vortex ring. The instantaneous vorticity fields for different values of Reynolds number (Gr_f and Pr are fixed) are shown in figure 4 and in figure 5. We see that transformation of the vortex structure is a gradual process, when we increase Re from 15.6 to 21.1 the radial inflow has already the dominant direction but still comes close to the center. After further increasing of Re up to 32.3 we achieve a state with localized at some radius vortex (figure 5). The radial inflow changes its direction (not periodically) so location of the vortex shown in figure 5 also changes. Figure 6 shows that locations of the center of the vortex for the stable case are concentrated near the axis of rotation but for unstable case they are dispersed at larger radii. For illustration of the flow structure at higher values of Re and Gr_f we used working fluid with lower viscosity (2.8 cSt instead of 5.1 cSt as in most of described experiments). For the fixed rotation rate and heating power it leads to increasing of Re and Gr_f and further destabilization of the flow. The flow becomes more chaotic with one or several vortices of different size (figure 7). Concluding the description of the vortex instability we want to emphasize two important features of the vortex evolution. The first one is that the instability of the vortex is tightly connected with changing structure of the radial inflow so the study of this process requires 3D approach. Another essential feature of the described evolution of the cyclonic vortex is its strong dependence on Re. We present map of regimes in figure 8 which clearly shows that there is critical value of rotational Reynolds number $Re \approx 23$ for the cyclonic vortex instability.

3.2. Modeling of latent heat release

Here we present first experiments on modeling of latent heat release using on-line PIV data processing. Modeling of latent heat release requires consideration of initial development stage of cyclonic vortex when increasing of radial velocity results in increasing of heat release. For the

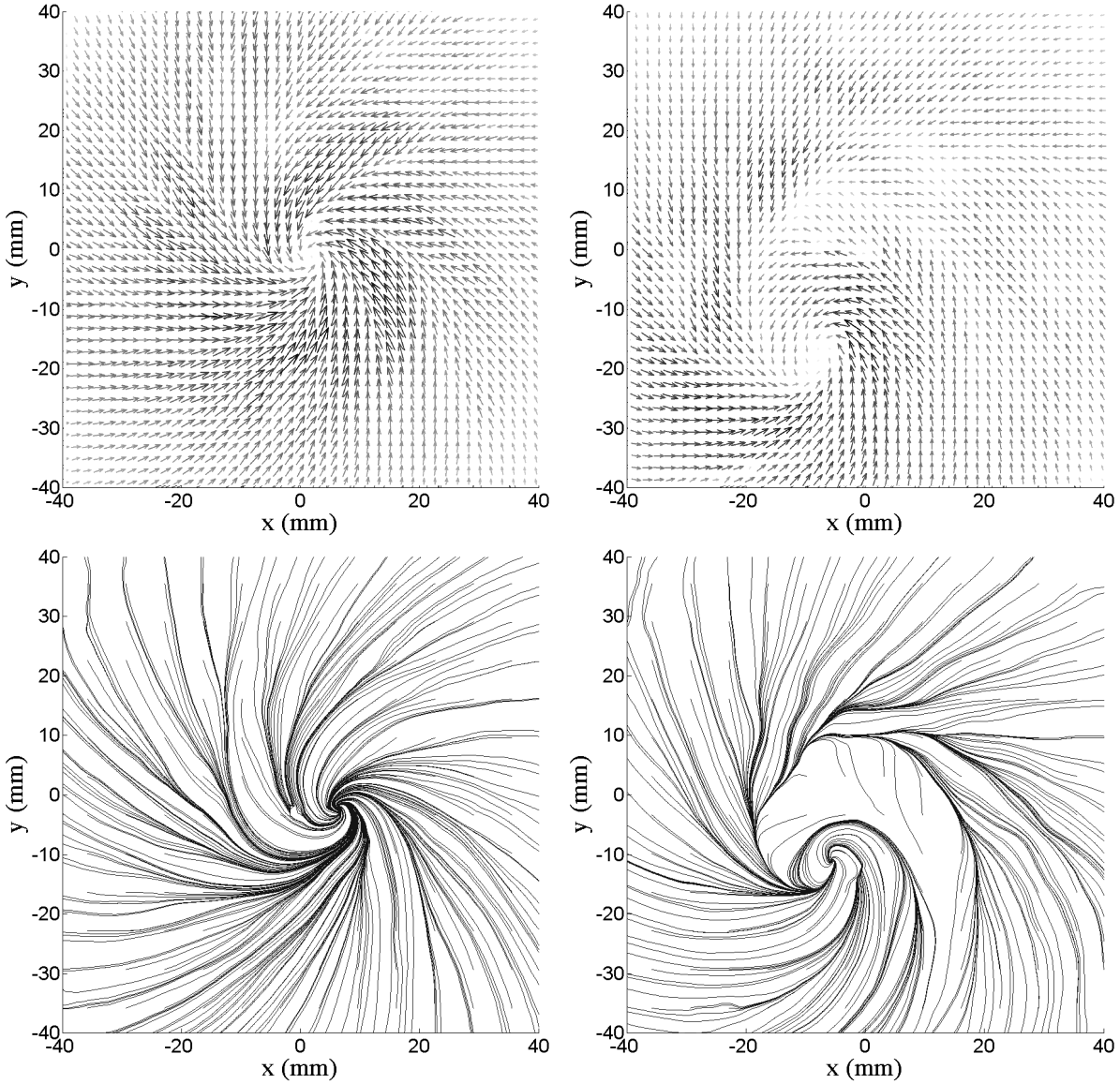

Figure 3. Instantaneous vector velocity fields (upper panel) and streamline flow fields (lower panel), left - $Re = 14.7$, right - $Re = 30.6$, $Gr_f = 6 \cdot 10^6$, $z = 3$ mm.

presented experiments linear dependence of heat flux on instantaneous mean radial velocity V_r is chosen in the following form, $P = P_0 V_r / V_{r,st}$, where P_0 is a maximal heating power and $V_{r,st}$ is a mean radial velocity for a quasi-stationary state with fixed heating power equal to P_0 as in [11]. According to the chosen dependence between radial velocity and heat flux it is expected that in case of monotonic increase of radial velocity a quasi-stationary state as in a case of constant heating power would be achieved. Intensive processes of heat and mass transfer take place in the boundary layer of tropical cyclone so 2D PIV measurements are done approximately in the middle of radial inflow at $z = 5mm$. The final size of the interrogation area was 16×16 pixels which allows to obtain 113×110 velocity vectors in the field of measurements. Only velocity vectors located over heating area are used for calculation of V_r (about two thousand vectors). Three series of measurements are carried out. The only difference between them is the value of angular velocity Ω. Now let us describe the course of the experiments. At first the solid-

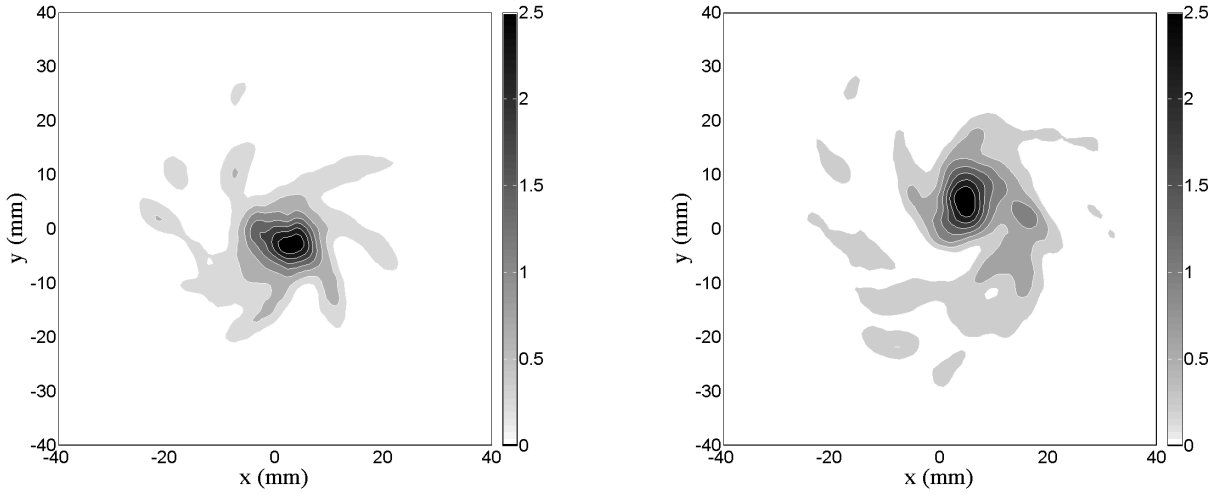

Figure 4. Instantaneous vorticity fields (s^{-1}), a - $Re = 14.7$, b - $Re = 30.6$, $Gr_f = 6 \cdot 10^6$, $z = 3$ mm.

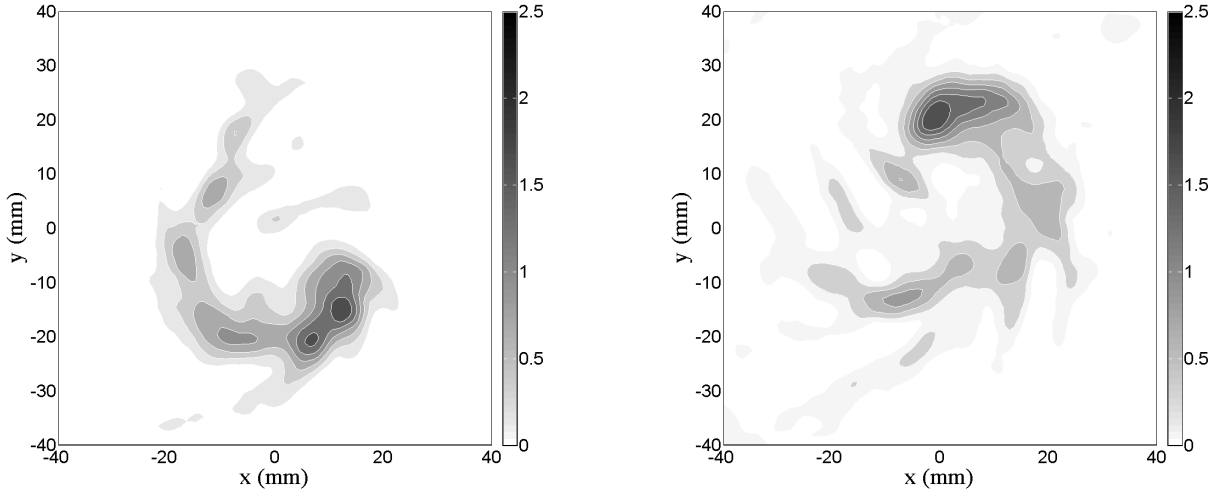

Figure 5. Two instantaneous vorticity fields (s^{-1}) for $Re = 30.6$, $Gr_f = 6 \cdot 10^6$, $z = 3$ mm.

body rotation of the fluid layer is achieved. Then for initiation of radial motion the heating is switched on (approximately 30% of a maximal value) for a short time (30 seconds). After that linear dependence between heating power and mean radial velocity is assigned.

At first we analyze the temporal evolution of heating power P and ΔT which is imposed temperature difference between temperature of the fluid (measured in the middle of the layer, near periphery, and temperature of the heater. There is important distinction between the role of heat release and horizontal temperature difference. The main source that leads to the formation of concentrated cyclonic vortex is radial inflow which transports additional angular momentum to the centre. In our case the radial inflow is driven mainly by convection which depends on ΔT so for the vortex development it is necessary that heat release leads to the increasing of ΔT. It is possible that large-scale flow effectively removes released heat by advection from the centre to the periphery. In that case ΔT becomes constant or decreases and this is the end of the cyclonic

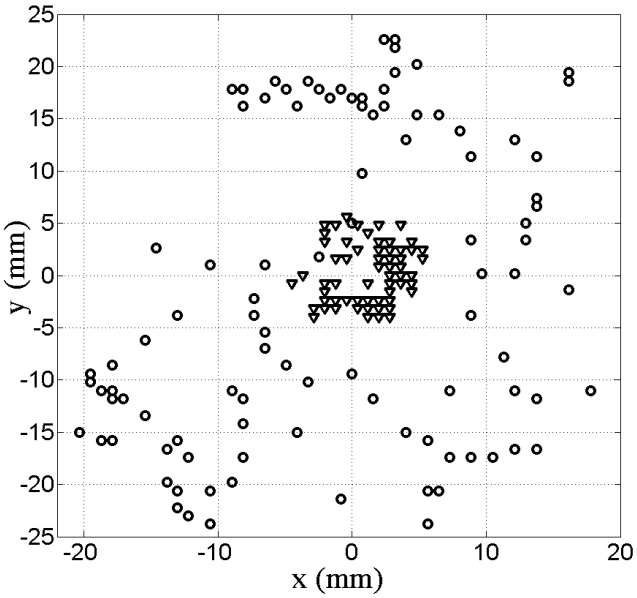

Figure 6. Locations of the cyclonic vortex center, triangles - $Re = 14.7$, circles - $Re = 30.6$, $Gr_f = 6 \cdot 10^6$, $z = 3$ mm.

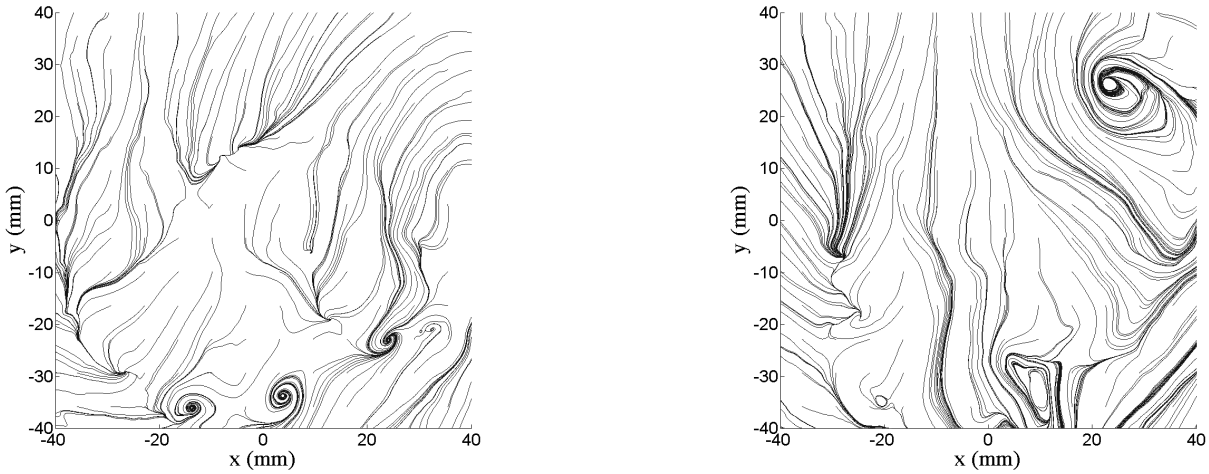

Figure 7. Instantaneous streamline flow fields (a,b) for $Re = 46$, $Gr_f = 1.4 \cdot 10^7$, $z = 3$ mm.

vortex intensification stage. Fig. 9 shows temporal evolution of the heating power and horizontal temperature difference for the three experiments. Please note that due to substantial level of fluctuations which are natural for convective flows with localized heating [16, 17, 18] we calculate and present in Fig. 9 (and others) a moving average of flow characteristics. For the comparison between time variation of P and ΔT they are normalized by their maximum values achieved for $\Omega = 0.17$ rad/s ($P_{max} = 55.6$ W, $\Delta T_{max} = 21.4°$). Short-time initial heating explains non-zero starting values of ΔT. We can see in Fig. 9 that up to some moment heating power which is proportional to the mean radial velocity leads to the increasing of ΔT which by-turn increases

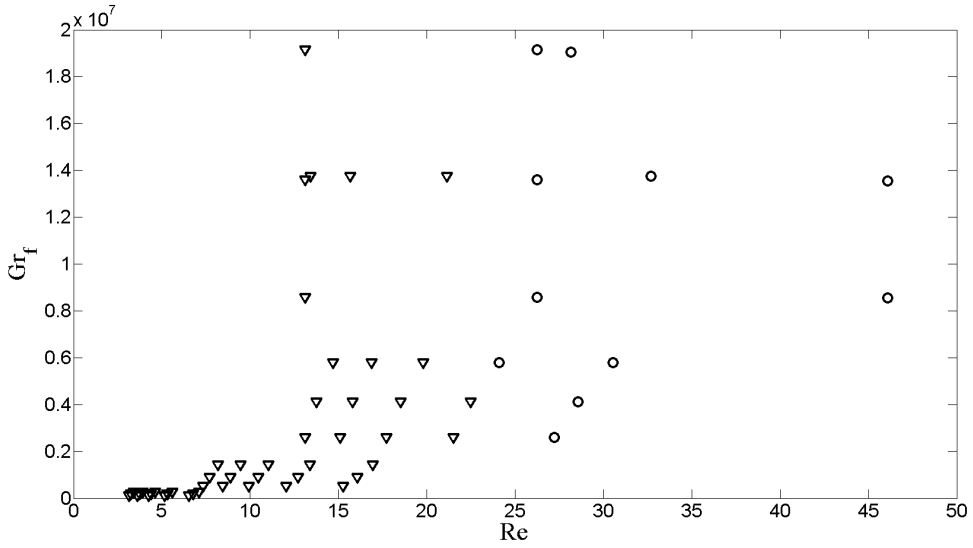

Figure 8. Map of regimes. Experiments with stable cyclonic vortex which is localized in the center are shown by triangles, experiments with unstable vortical flows are shown by circles.

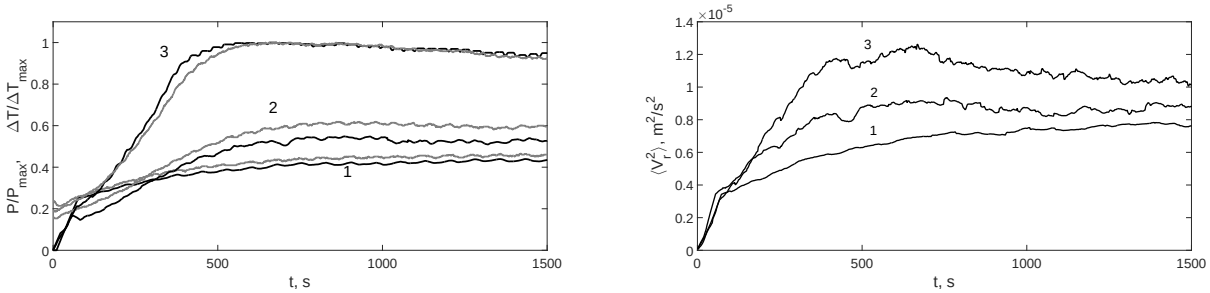

(a) (b)

Figure 9. a – normalized dependences of heating power P (black lines) and temperature difference ΔT (grey lines); b – temporal evolution of the mean square radial velocity; 1 – $\Omega = 0.08$ rad/s, 2 – $\Omega = 0.11$ rad/s, 3 – $\Omega = 0.17$ rad/s.

radial inflow. This is development stage of the cyclonic vortex. Finally when most of the heating power is removed from the heater by flow circulation ΔT achieves its maximum value and vortex development is stopped. It is interesting that unlike [10, 11, 12] where heat flux was constant, here the achieved heating power which is proportional to the mean radial velocity is highest for the relatively fast rotation rate. It proves that linkage between flow circulation and heat release is of primary importance for the vortex development.

Important characteristics of the cyclonic vortex are energies of radial and azimuthal flows. For the presented experiments they increase with increasing of Ω (Fig. 9 and Fig. 10). Comparison between values of mean square velocities of radial and azimuthal flows $\langle V_r^2 \rangle$ and $\langle V_a^2 \rangle$ show that for $\Omega = 0.08$ rad/s energy of radial flow is higher than energy of azimuthal flow, for $\Omega = 0.11$ rad/s they are comparable and for $\Omega = 0.17$ rad/s azimuthal flow is much more intensive. For $\Omega = 0.17$ rad/s there is monotonic increase of $\langle V_a^2 \rangle$ when both ΔT and P decrease. It can be explained by specifics of the presented experiment. The cooling of the fluid is provided by the heat release to the relatively cold air at the open surface. It depends on the temperature of the

fluid and during the non-stationary stage of experiment the overall heat flux is not zero and mean temperature of the fluid increases. It leads to the change of physical properties of the fluid mainly of kinematic viscosity. Decreasing of kinematic viscosity has influence on the processes in the boundary layer and increases $\langle V_a^2 \rangle$. Taking into account the described kinematic viscosity, variation $\langle V_a^2 \rangle$ can be corrected:

$$\langle V_a^2 \rangle_{corr} = \langle V_a^2 \rangle \cdot (\nu/\nu_0)^2, \tag{4}$$

where ν_0 is the original value of kinematic viscosity. It is evident that temporal evolution of $\langle V_a^2 \rangle_{corr}$ is similar to ΔT variation (Fig. 10). This strong correlation makes possible to control the intensity of the cyclonic vortex by variation of ΔT. The last interesting observation concerns similarity of the dynamics of maximum values of radial and azimuthal velocities. Temporal evolution of normalized values of $V_{r,max}$ and $V_{a,max}$ is presented in Fig. 10. We can see that despite large quantitative differences the temporal evolution is definitely similar and it can be a ground for a simple mathematical model which would describe the vortex formation in a presented system.

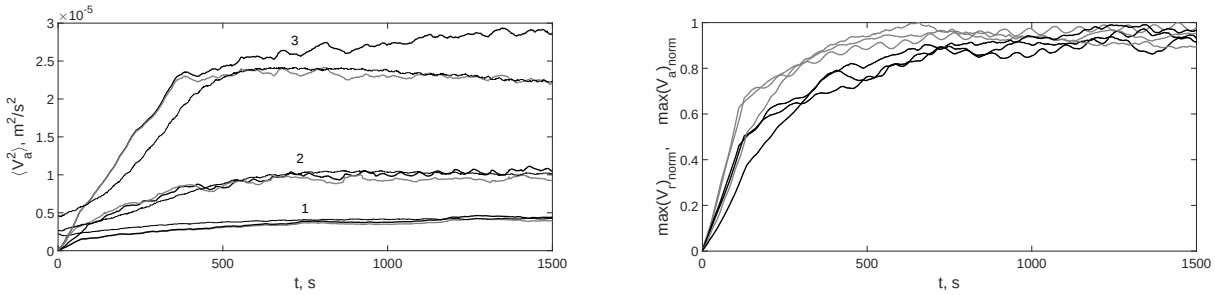

(a) (b)

Figure 10. a – temporal evolution of the mean square azimuthal velocity, thick black line – the mean square azimuthal velocity, thick grey line - corrected mean square azimuthal velocity, thin black line - normalized ΔT; 1 – $\Omega = 0.08$ rad/s, 2 – $\Omega = 0.11$ rad/s, 3 – $\Omega = 0.17$ rad/s; b – temporal evolution of normalized maxima of radial (grey lines) and azimuthal (black lines) velocity.

4. Conclusions

The laboratory analog of TC is stable in a limited interval of rotational Reynolds number. The instability of the vortex is tightly connected with a structure of the radial inflow. Up to moderate values of rotational Reynolds number the radial flows consist of several branches which transport angular momentum to the center. When Re exceeds the critical value radial inflow changes its structure and appears as one wide branch which does not reach the center. As a result the vortex which slowly moves around the center is formed instead of the vortex localized in the center. Further increase of Re leads to the chaotic state with several vortices which appear at different locations near the periphery of the heating area. The narrow interval of existence of localized intensive cyclonic vortex explains small number of laboratory studies of large-scale atmospheric vortices such as tropical cyclones. Also we assume that if described instability takes place in real tropical cyclones it can be a reason why from a multiple cases of large-scale vortical disturbances in a favourable environment only a few can become a tropical cyclone.

The laboratory modeling of latent heat release on the base of controlled forcing is described. A series of experiments with laboratory analog of tropical cyclone using feedback between velocity and a heating is carried out. To our knowledge this is the first attempt since [19]. It is known

that convection and formation of secondary (meridional) circulation is of primary importance for tropical cyclone (TC) formation [6, 7]. We show that for laboratory model of TC the crucial parameter which defines the mean radial velocity and intensity of the vortex is imposed temperature difference ΔT. Strong dependence of developed vortex intensity on rotation rate is found. It gives a reason to assume that development of real TCs also substantially depends on the intensity of initial vortical disturbance. The similarity between temporal dynamics of maximum values of radial and azimuthal velocities for different rotation rates despite their large quantitative discrepancies shows that there is some universal feature of the development stage of cyclonic vortex with localized heat flux. It can serve as a ground for a simple analytical model of cyclonic vortex dynamics. Finally we can conclude that the linkage between velocity and heat release is of crucial importance for the cyclonic vortex formation. This is only the first step toward the solution of the problem of latent heat release in such a complex system as tropical cyclone and different functional dependences of heat release on flow characteristics will be studied further.

Acknowledgments

The financial support of grant RFBR No.17-45-590846 is gratefully acknowledged. Computing resources of the supercomputer "Triton" were provided by Center of Shared Facilities (Institute of Continuous Media Mechanics UrB RAS).

References

[1] Kilroy G and Smith R K 2015 *Quarterly Journal of the Royal Meteorological Society* **141** 714–726
[2] Etling D and Brown R 1993 *Boundary-Layer Meteorology* **65** 215–248
[3] Foster R 2013 *Oceanography* **26** 58–67
[4] Moon Y and Nolan D S 2015 *Journal of the Atmospheric Sciences* **72** 164–190
[5] Moon Y and Nolan D S 2015 *Journal of the Atmospheric Sciences* **72** 191–215
[6] Emanuel K 2003 *Annual Review of Earth and Planetary Sciences* **31**
[7] Montgomery M T and Smith R K 2017 *Annual Review of Fluid Mechanics* **49** 541–574
[8] Gall R, Franklin J, Marks F, Rappaport E N and Toepfer F 2013 *Bulletin of the American Meteorological Society* **94** 329–343
[9] Bogatyrev G P 1990 *Soviet Journal of Experimental and Theoretical Physics Letters* **51** 630
[10] Batalov V, Sukhanovsky A and Frick P 2010 *Geophysical and Astrophysical Fluid Dynamics* **104** 349–368
[11] Sukhanovskii A, Evgrafova A and Popova E 2016b *Quarterly Journal of the Royal Meteorological Society* **142** 2214–2223
[12] Sukhanovskii A, Evgrafova A and Popova E 2017 *Dynamics of Atmospheres and Oceans* **80** 12–28
[13] Shchapov V, Evgrafova A, Masich G, Pavlinov A, Popova E, Sukhanovskii A and Chugunov D 2018 *Program Systems: Theory and Applications (in Russian)* **9** 3–19
[14] Zhang J A, Rogers R F, Nolan D S and Marks Jr F D 2011 *Monthly Weather Review* **139** 2523–2535
[15] Bogatyrev G 2009 *Laboratory model of a tropical cyclone (in Russian)* (Perm)
[16] Boubnov B and Van Heijst G 1994 *Experiments in fluids* **16** 155–164
[17] Maza D, Vallone A, Mancini H and Boccaletti S 2000 *Physical review letters* **85** 5567
[18] Sukhanovskii A, Evgrafova A and Popova E 2016a *Physica D: Nonlinear Phenomena* **316** 23–33
[19] Hadlock R K and Hess S L 1968 *Journal of the Atmospheric Sciences* **25** 161–177